Surface Charge-Density Wave on the One-Dimensional Organic Conductor β-(BEDT-TTF)2PF_6

Masahiko Ishida,[1] Takehiko Mori,[2] and Hidemi Shigekawa[1,3,*]

[1]*Institute of Applied Physics, CREST, Japan Science and Technology Corporation (JST), University of Tsukuba, Tsukuba 305-8573, Japan*

[2]*Department of Organic and Polymeric Materials, Tokyo Institute of Technology, Tokyo 152-8552, Japan*

[3]*Department of Chemistry and Biotechnology, Graduate School of Engineering, The University of Tokyo, Hongo, Tokyo 113-8656, Japan*

(Received 2 April 1999)

We performed STM and theoretical studies of the surface of β-(BEDT-TTF)$_2PF_6$ which is known to show a metal-insulator transition at 297 K with the nesting vector of $Q_{\text{bulk}} = a^* + 0.5c^*$ as a bulk phase. Two typical charge-density wave (CDW) phases with $Q_{S1} = 0.13a^* + 0.26c^*$ and $Q_{S2} = 0.19a^* + 0.20c^*$ were observed at 285 K on the surface. The observed structures were correlated well with the analysis of the susceptibility $\chi(Q)$, given the incomplete surface-charge transfer in the polar surface of this material. This is the first observation of surface CDW phases that reflect the characteristics of the electronic structure. These results suggest the possible discovery of other surface properties, such as surface superconductivity, in organic materials with a polar surface.

PACS numbers: 71.45.Lr, 61.16.Ch, 71.15.Fv, 73.20.Dx

Charge-density waves (CDWs), formed in low-dimensional conductors, have attracted considerable attention recently due to their relation to the metal-insulator (MI) phase transitions in strongly correlated electronic systems. In order to understand the characteristic properties of CDWs, information about their local structures is extremely important. As a result, numerous studies have been performed using scanning tunneling microscopy (STM) and related techniques [1–6]. For example, from a local spectroscopic study of the CDW phases of the TaS_xSe_{2-x}, MI transition due to the Mott-Hubbard localization was directly shown on an atomic scale, and analyzed with respect to the band structure [3]. Recently, a STM study was performed on the surface of a quasi-one-dimensional organic conductor, tetrathiafulvalene-tetracyanoquinodimethane (TTF-TCNQ), and the incommensurate $2k_F$ CDW, driven by Peierls instability, was directly observed in real space with molecular resolution [4]. Thus, interesting characteristics have been successfully observed, as described. However, despite the early expectations, the CDW phases observed on surfaces have been understood to be identical to those in the bulk states. For example, the modulated CDW phase observed on the $1T$-TaS_2 surface was explained by the structure of bulk phases [5]. Furthermore, a specific structure observed on the TTF-TCNQ surface, i.e., a CDW chain aligned along the a axis with an anomalous rise in the tunneling current, was attributed to be the result of local perturbation due to impurities or surface defects [4]. Basically, no surface CDW phases which have characteristics which differ from the bulk phase have previously been observed.

On the other hand, bis(ethylenedithio)tetrathiafulvalene (BEDT-TTF)-based organic compounds are distinct from other low-dimensional materials with respect to their surface molecule ionicity. These materials consist of alternately stacked BEDT-TTF and anion layers (Fig. 1), and 0.5 electrons transfer from each BEDT-TTF molecule to the anion layers, which makes the BEDT-TTF and anion layers conductive and insulating, respectively. Therefore, a surface terminated with either a BEDT-TTF or cation layer begins to exhibit characteristics of a polar surface. On the polar surface, the net surface charge is adjusted to cancel the potential gradient throughout the crystal. Such a change is expected to have considerable influence on surface geometric and electronic structures. In fact, recent studies revealed that surface reconstruction was induced on the molecular crystal surface of BEDT-TTF compounds [7]. These results again raise interest in the study of the phase transitions induced in the surface layers. Since the charge transfer is incomplete in the BEDT-TTF molecular layer terminating the surface, a change in the band filling is expected to significantly influence the characteristic properties such as the CDW, on the surface.

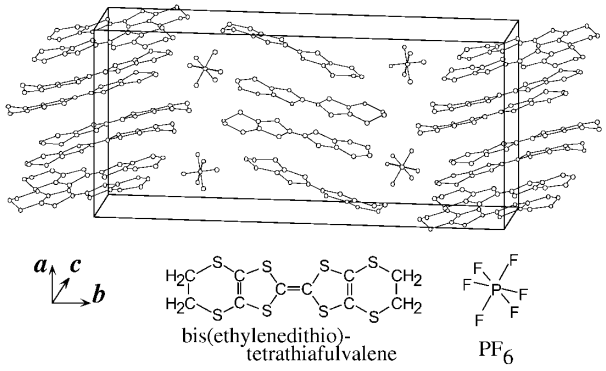

FIG. 1. Crystal structure of β-(BEDT-TTF)$_2PF_6$ determined by x-ray diffraction ($a = 1.4960$, $b = 3.2643$, $c = 0.6664$ nm).

 0031-9007/99/83(3)/596(4)$15.00

From the standpoint described, we performed STM and theoretical studies on β-(BEDT-TTF)$_2$PF$_6$ [8]. This material is the first organic conductor recognized as one dimensional along the side-by-side (transverse) array. The largest conductivity is exhibited parallel to the molecular plane (the c axis in Fig. 1), and this salt undergoes a MI transition at 297 K. Below this temperature the emergence of a twofold modulation along the conductive c axis was confirmed by x-ray diffraction [9]. On the basis of ESR measurements [8], spin susceptibility measurements [9], and tight-binding energy band calculations [10], the twofold modification is understood to be a MI transition associated with $2k_F$ CDW. Single crystals of β-(BEDT-TTF)$_2$PF were grown by the standard electrochemical oxidation method and then fixed to metallic plates with conductive silver epoxy. The STM measurements were performed on the crystal a-c plane terminated with the BEDT-TTF molecular layer (Fig. 1) in a constant-height mode under ultrahigh-vacuum conditions using electrochemically etched tungsten tips. Sample temperatures ranged from ~80 K to room temperature, and were measured using a calibrated thermocouple placed near the sample holder.

At temperatures above 290 K, BEDT-TTF molecular rows were observed without any additional structures. This indicates that the metallic phase remains even below the transition temperature, ~297 K. Since the CDW phase was observed above the transition temperature in the case of TTF-TCNQ [4], the transition to the CDW phase may have been slightly disturbed on the surface of this material, suggesting a difference from the bulk phase. At temperatures below 280 K, it was difficult to observe a detailed surface structure because of the considerable reduction in conductivity [8].

In the temperature range from 280 to 290 K, however, new structural modulations along the molecular rows emerged on the surface. Figures 2(a) and 2(b) show the two typical superstructures stably observed on the surface at 285 K. In these images, the molecular rows along the c axis are arrayed with a separation of ~1.5 nm in the a-axis direction. This value of separation corresponds well with the lattice constant of 1.49 nm in the a axis. Moreover, noteworthy features exist in the structure of molecular rows in these images. Figures 2(c)–2(e) show the schematic structures of the bulk CDW phase and the two observed superstructures in Figs. 2(a) and 2(b).

First, the observed structures have considerably larger modulations compared to the structure of the bulk CDW phase that has a twofold modulation along the c axis. The new lattice constants observed along the c axis are 2.6 ± 0.1 nm [Fig. 2(a)] and 3.3 ± 0.05 nm [Fig. 2(b)], and are close to fourfold and fivefold longer, respectively, than the original lattice constant of 0.67 nm. A second interesting feature of the modulated structures is the phase shift. As the schematic in Fig. 2(c) shows, according to both experimental and theoretical studies, the bulk CDW

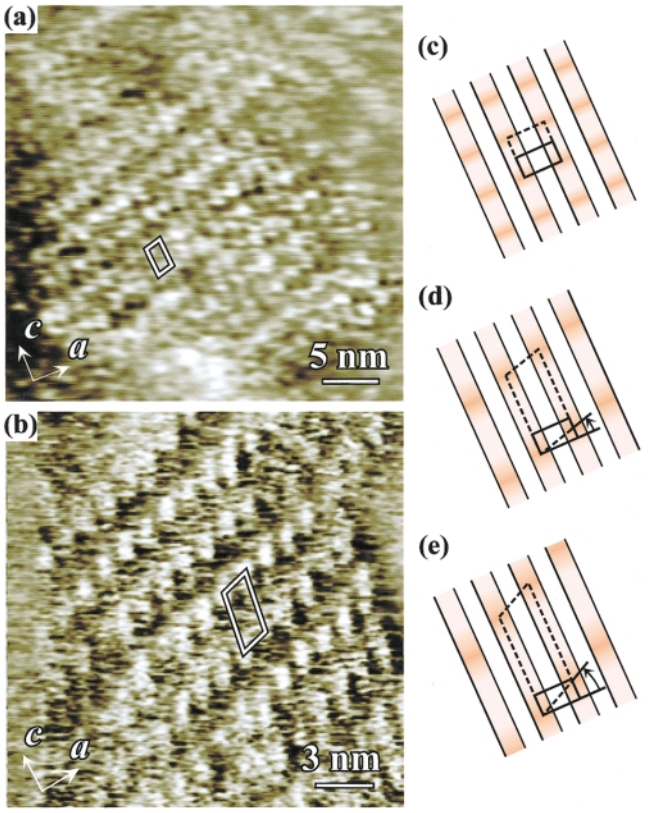

FIG. 2 (color). (a),(b): STM images obtained on the a-c plane of β-(BEDT -TTF)$_2$PF $_6$ at 285 K (V_t = 1.0 V , I_t = 0.3 nA). (c)–(e) are schematic models of the bulk CDW and the observed superstructures of (a) and (b), respectively. Original and the observed unit cells are represented by solid and dotted lines in (c)–(e), respectively.

phase does not exhibit periodic modulations along the a axis. On the other hand, the observed structures exhibit periodic modulations along the a axis, as shown in Figs. 2(d) and 2(e). Their periodicities along the a axis are 11 ± 1 nm and 8.0 ± 0.7 nm, and are close to sevenfold–eightfold and fivefold longer than the a-axis lattice constant, respectively. Therefore, they are completely different from the structure of the bulk CDW phase determined by x-ray diffraction. However, these structures emerged only below the critical temperature of MI transition. As is known, the formation of CDW depends strongly on the geometry of the Fermi surface (FS), i.e., the degree of FS nesting. Therefore, in order to understand the observed modulations, we calculated the energy band structure using the tight-binding approximation. The parameters for the tight-binding calculation of the two-dimensional cation (BEDT-TTF) sheet were estimated from the overlaps of the highest-occupied molecular orbitals (HOMOs) of the neighboring cations [11]. According to STM and atomic-force microscopy (AFM) studies, the displacement of the surface molecules from the crystal structure was estimated to be 0.02 nm at most, which is not very large with respect to the molecular size of

~1.4 nm. Therefore, we adopted the overlap parameters of the bulk crystal for the calculation [10].

The primary factor that governs the FS geometry is the change in the band filling [6]. Band filling of the charge-transfer molecular crystal depends on the amount of molecular charge. In the case of β-(BEDT-TTF)$_2$PF$_6$, if the charge transfer is completed, the BEDT-TTF molecules which organize the conductive band retain a uniform positive charge of $\delta = 0.5$. For the surface layer, however, the molecular charge is reduced to $\delta' = 0.25$ due to the missing anion layer on one side. Therefore, the HOMO band filling in the surface layer changes from 6/8 (half filled as represented by a hole in the upper band) to 7/8 (quarter filled).

Figure 3(a) shows the calculated HOMO band structure, where the two marked Fermi levels have been determined by taking into account the change in the molecular charge between the bulk and the surface layer. The structure of the FSs corresponding to the bulk and the surface Fermi levels is shown in Fig. 3(b) by the solid and dotted lines, respectively. The FSs are depicted using the extended zone scheme with regard to the degeneracy on X-U. As shown in Fig. 3(b), the FSs in the bulk layer have a sinusoidal shape and can be nested by the transfer vector depicted by Q_{bulk}. The change in the Fermi level results in two major changes in the geometry of the FS as shown in Fig. 3(b): (1) closer distance between the neighboring FS sheets, and (2) a nonsinusoidal shape of the FS. While the former change clearly indicates a longer periodic modulation in real space, the latter complicates the estimation of the desired nesting vector. In order to clarify this point, we calculated the susceptibility $\chi(Q)$ for the bulk and the surface layer, which represents the degree of FS nesting resulting in the formation of CDW phase [12,13].

Figure 4 shows the contour plot of $\chi(Q)$ with bulk-phase band filling, the structure of which is characterized by the steep increase of $\chi(Q)$ around $Q_{\mathrm{bulk}} = a^* + 0.5c^*$. The inset in Fig. 4 shows the structure of FS nesting. The solid line in Fig. 4 represents the FS translated by the vector Q_{bulk} from the lower side, which is perfectly nested with the original FS in the upper side, represented by the dashed line. This result agrees well with the twofold CDW structure shown along the c axis, which was determined by x-ray diffraction for the bulk phase. On the other hand, Fig. 5(a) shows the contour plot of $\chi(Q)$ with surface-phase band filling. The structure of $\chi(Q)$ differs markedly from that in Fig. 4: the peak became broader and its position shifted toward the smaller Q_c direction. The nesting vector, which corresponds to the peak position, is $Q_{\mathrm{surf}} = a^* + 0.27c^*$, which is expected to produce a 3.7-fold periodic modulation along the c axis. However, as shown in the inset of Fig. 5(a), the nesting vector Q_{surf} does not perfectly nest the FS sheets, suggesting, i.e., the possibility of the appearance of other CDW phases, as observed experimentally. The incompleteness of FS nesting is the result of the nonsinusoidal shape of the FS, which makes the $\chi(Q)$ peak broader because partial nesting of FS sheets is expected around the Q_{surf}. Therefore, as shown in Fig. 5(a), $\chi(Q)$ does not decrease steeply and has a relatively high susceptibility even around the peak position, and particularly along the two ridge lines denoted by the dotted lines.

In Fig. 5(a), the wave numbers corresponding to the experimentally obtained periodic modulations in Figs. 2(a) and 2(b) are marked by $Q_{S1} = 0.13a^* + 0.26c^*$ and $Q_{S2} = 0.19a^* + 0.20c^*$, respectively. They are located around the ridge lines described above, and have relatively high values of $\chi(Q)$. In addition, their periodicities along the c axis are 2.6 ± 0.1 nm and 3.3 ± 0.05 nm, and are close to being commensurate with the underlying lattice; fourfold and fivefold, respectively. Furthermore, the STM observations were performed near the critical temperature.

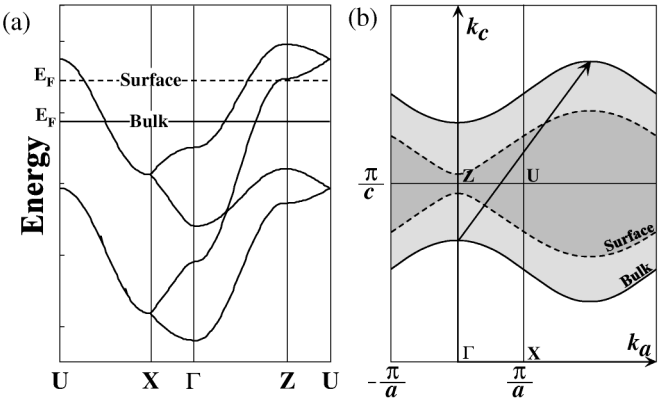

FIG. 3. (a) Calculated HOMO band structure and (b) the structure of the FSs corresponding to the bulk (solid line) and the surface (dotted line) Fermi levels shown in (a).

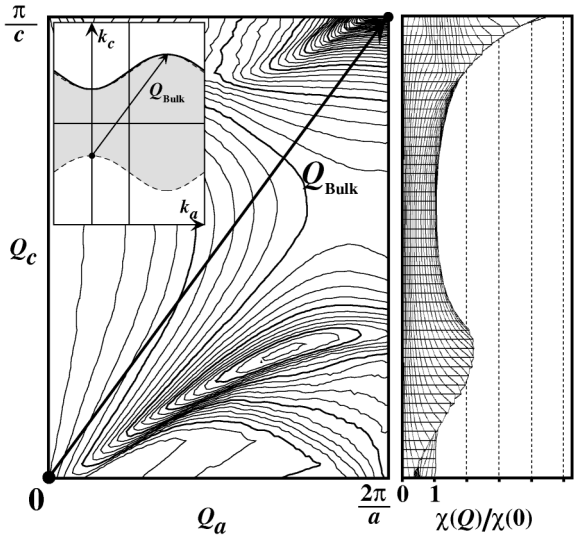

FIG. 4. Contour plot and side view of $\chi(Q)$ with bulk-phase band filling (see text).

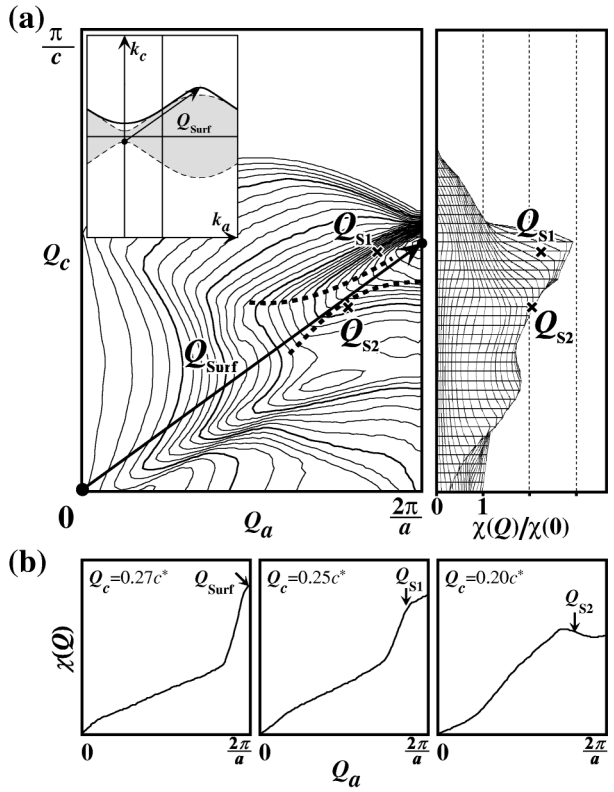

FIG. 5. (a) Contour plot and side view of $\chi(Q)$ with surface-phase band filling. Q_{S1} and Q_{S2} are the nesting vectors corresponding to the observed CDW phases in Figs. 2(a) and 2(b), respectively. (b) Cross sections of $\chi(Q)$ in (a) along $Q_c = 0.27c^*$, $0.25c^*$, and $0.20c^*$.

Therefore, the incommensurate CDW expected from the Q_{surf} is not stable enough to be observed due to the sliding motion over the underlying lattice, and the commensurate CDW phases, such as the observed Q_{S1} and Q_{S2}, might have been realized.

Next, we consider the modulation along the a axis. Figure 5(b) shows the cross sections of $\chi(Q)$ along $Q_c = 0.27c^*$, $0.25c^*$, and $0.20c^*$. As shown in Fig. 5(b), vectors $Q_{S1} = 0.13a^* + 0.26c^*$ and $Q_{S2} = 0.19a^* + 0.20c^*$ are located near the peaks and have high $\chi(Q)$ values. Therefore, the observed CDW phase shift is also consistent with the calculation. Instability induced in the surface layer might have caused the phase shift between two CDW chains, as it did in the CDW structure of the TTF-TCNQ crystal. Further study is necessary to clarify the interaction between CDW chains.

In summary, we performed STM and theoretical studies of the surface of β-(BEDT-TTF)$_2$PF$_6$ which is known to show a MI transition at 297 K with the nesting vector of $Q_{bulk} = a^* + 0.5c^*$ as a bulk phase. Two typical CDW phases with $Q_{S1} = 0.13a^* + 0.26c^*$ and $Q_{S2} = 0.19a^* + 0.20c^*$ were observed at 285 K on the surface. The observed structures were well correlated with the analysis of the susceptibility $\chi(Q)$ in consideration of the incomplete surface-charge transfer in the polar surface of this material. This is the first observation of surface CDW phases which reflects the characteristics of the surface electronic structure. Furthermore, slightly lowered transition temperature and the nonsinusoidal FS sheet in the surface layer suggested interference of the FS nesting. These results suggest the possible discovery of other surface properties, such as surface superconductivity, in organic materials with a polar surface.

This work was supported by a Grant-in-Aid for Scientific Research from the Ministry of Education, Science, Sports and Culture of Japan. One of the authors (M. I.) was financially supported by the Japan Society for the Promotion of Science (JSPS).

*Email address: hidemi@ims.tsukuba.ac.jp (http://dora.ims.tsukubas.ac.jp)

[1] R. V. Coleman, B. Drake, P. K. Hansma, and G. Slough, Phys. Rev. Lett. **55**, 394 (1985).
[2] E. Meyer, R. Wiesendanger, D. Anselmetti, H. R. Hidber, H.-J. Guntherodt, F. Levy, and H. J. Berger, Vac. Sci. Technol. **A8**, 495 (1990).
[3] J.-J. Kim, W. Yamaguchi, T. Hasegawa, and K. Kitazawa, Phys. Rev. Lett. **73**, 2103 (1994).
[4] T. Nishiguchi, M. Kageshima, N.-A. Kato, and A. Kawaze, Phys. Rev. Lett. **81**, 3187 (1998).
[5] B. Burk, R. E. Homson, J. Clarke, and A. Zettl, Science **257**, 362 (1992).
[6] X. L. Wu and C. M. Lieber, J. Am. Chem. Soc. **110**, 5200 (1988).
[7] M. Ishida, K. Miyake, K. Hata, and H. Shigekawa, Phys. Rev. B **55**, 6773 (1997).
[8] H. Kobayashi, R. Kato, T. Mori, A. Kobayashi, Y. Sasaki, G. Saito, and H. Inokuchi, Chem. Lett. **1983**, 759 (1983).
[9] G. K. R. Senadeera, T. Kawamoto, T. Mori, J. Yamaura, and T. Enoki, J. Phys. Soc. Jpn. **67**, 4193 (1998).
[10] T. Mori, A. Kobayashi, Y. Sasaki, R. Kato, and H. Kobayashi, Solid State Commun. **53**, 627 (1985).
[11] T. Mori, A. Kobayashi, Y. Sasaki, H. Kobayashi, G. Saito, and H. Inokuchi, Bull. Chem. Soc. Jpn. **57**, 627 (1984).
[12] N. J. Doran, J. Phys. C **11**, L959 (1978).
[13] G. Montambaux, *Low-Dimensional Conductors and Superconductors* (Plenum, New York, 1987), p. 233.